OPEN

Microsystems & Nanoengineering (2015) 1, 15025; doi:10.1038/micronano.2015.25

www.nature.com/micronano

ARTICLE

Transient thermal response of micro-thermal conductivity detector (μTCD) for the identification of gas mixtures: An ultra-fast and low power method

Alireza Mahdavifar[1], Milad Navaei[1], Peter J. Hesketh[1], Melvin Findlay[2], Joseph R. Stetter[2] and Gary W. Hunter[3]

Micro-thermal conductivity detector (μTCD) gas sensors work by detecting changes in the thermal conductivity of the surrounding medium and are used as detectors in many applications such as gas chromatography systems. Conventional TCDs use steady-state resistance (i.e., temperature) measurements of a micro-heater. In this work, we developed a new measurement method and hardware configuration based on the processing of the transient response of a low thermal mass TCD to an electric current step. The method was implemented for a 100-μm-long and 1-μm-thick micro-fabricated bridge that consisted of doped polysilicon conductive film passivated with a 200-nm silicon nitride layer. Transient resistance variations of the μTCD in response to a square current pulse were studied in multiple mixtures of dilute gases in nitrogen. Simulations and experimental results are presented and compared for the time resolved and steady-state regime of the sensor response. Thermal analysis and simulation show that the sensor response is exponential in the transient state, that the time constant of this exponential variation was a linear function of the thermal conductivity of the gas ambient, and that the sensor was able to quantify the mixture composition. The level of detection in nitrogen was estimated to be from 25 ppm for helium to 178 ppm for carbon dioxide. With this novel approach, the sensor requires approximately 3.6 nJ for a single measurement and needs only 300 μs of sampling time. This is less than the energy and time required for steady-state DC measurements.

Keywords: gas sensor; MEMS; micro-bridge; micro-heater; μTCD; thermal conductivity sensor; transient heat transfer modeling

Microsystems & Nanoengineering (2015) **1,** 15025; doi:10.1038/micronano.2015.25; Published online: 26 October 2015

INTRODUCTION

During the past four decades, gas sensors, detectors, and analyzers have been widely used to measure the composition of gas mixtures or to detect the presence of particular species in a gas medium[1]. Many conventional gas detectors are based on electrochemical or chemo-resistive effects. Despite providing good selectivity in some cases, the performance of these technologies is limited by the nature of the chemical adsorption/diffusion process of the chemical at the surface or through the sensing film. Therefore, many types of conventional sensors suffer from a slow response time and memory effect and require frequent recalibration. Instability and poor shelf-life are additional challenges for gas sensing[1]. Important characteristics of different gas sensor technologies are: selectivity, sensitivity, size and power consumption, response time, and hysteresis effects.

An electrothermal gas sensor works based on the interaction between heat generation in an electrically conductive suspended element and heat transfer from the element via the surrounding gas medium. When electrical power dissipation occurs in a suspended hot element, the thermal conductivity of the gas surrounding the device determines the rate of heat loss. As a result, the steady-state temperature of the hot element is a function of the gas ambient properties. If the heater is constructed from an electric conductor with a sufficiently high temperature coefficient of resistance (TCR) this allows the average temperature of the heater to be determined by measuring the change in resistance when heating occurs in different gas ambient mixtures. Conventional thermal gas detectors have been employed in the form of relatively small pellistors[2]. Pellistors are solid-state devices used to detect gases that are either combustible or exhibit significantly different thermal conductivity relative to air.

Along with the development of MEMS technology, microhotplates were developed to operate at lower power and are based on a similar principal as pellistors. Zanini *et al.*[3] fabricated a calorimetric microhotplate sensor using silicon micromachining techniques. The device output was found to be proportional to the concentration of combustible gas, in this case hydrogen and propylene. The smaller size of these micro-plates allowed them to reach operating temperatures as high as 500 °C in approximately 20 ms at a power level of 100 mW. An electric circuit consisting of a Wheatstone bridge with two external resistors and a reference sensor was used to measure the steady-state resistance of the microhotplate.

Suehle *et al.*[4,5] developed the first monolithic tin oxide gas sensor hotplate by commercial CMOS foundry fabrication. A response time of 200 s was observed for hydrogen detection and the device could achieve a temperature of 350 °C at 45 mW. Later Elmi *et al.*[6] developed smaller metal oxide microhotplates (50–120 μm in diameter) for detection of volatile organic compounds (VOCs). The sensors required 8.9 mW for detection. Decarli *et al.*[7] integrated a technique for the controlled deposition of nanostructured metal oxide films with MEMS-based microfabrication technologies to fabricate microhotplate gas sensors

[1]School of Mechanical Engineering, Georgia Institute of Technology, Atlanta, GA 30332, USA; [2]KWJ Engineering Inc., Newark, CA 94560, USA and [3]NASA Glenn Research Center, Cleveland, OH 44135, USA

Correspondence: Peter J. Hesketh (peter.hesketh@me.gatech.edu)

Received: 1 April 2015; revised: 1 September 2015; accepted: 2 September 2015

with tungsten and iron oxides. These metal oxide technologies exhibited a slow response time of several minutes.

Micro-thermal conductivity detector (μTCD) gas sensors, unlike calorimetric or metal oxide gas sensors, are based on changes in the thermo-physical properties of the surrounding gas and do not rely on gas adsorption and reaction with a catalyst or thin films. Therefore, measurements can be taken more rapidly and the sensor can be operated in a continuous manner and repeatedly used without memory effects. Puente *et al.*[8] demonstrated a thermal conductivity micro-sensor for measurement and analysis of natural gas composition. Miniature thermal conductivity gas sensors have been developed as detectors for gas chromatography (GC) systems in which very fast response is required for the detector. Cruz *et al.*[9] fabricated a μTCD for this purpose. The design included a platinum heater resting on a silicon nitride membrane. The total size of the membrane structure was larger than 0.5 mm and the sensors consumed approximately 1 W power at typical GC flow rates. To improve sensitivity, four TCDs in a Wheatstone bridge arrangement were exposed to the reference flow, and column effluent and samples of output voltage were taken under a DC input voltage.

Because electro-thermal sensors rely on heat transfer as the sensing mechanism, some researchers have explored the nature of the thermal phenomena through modeling and simulations. The efforts include thermal modeling of microheater gas flow sensors[10,11] and electrothermal simulation of μTCD for geometry optimization[9]. However, previous works relied on significant simplifications in handling the complexity of physics and geometry.

Despite advancements in the fabrication of μTCDs and efforts to make them smaller, the methods of measurement are relatively undeveloped and reported investigation of TCDs has been based on steady-state readings from a conventional Wheatstone bridge with DC excitation. The frequency method of 3ω (3 omega) and time domain thermo-reflectance (TDTR) have been used in other applications for measuring thermal conductivity in solids, and transient hot wires (THW) have been studied in some fluid samples[12,13]. Relatively large geometries used in these studies involve long settling times, losses, complex 3D isotherms, natural convection effects, and radiation. Moreover, a frequency analysis method requires a lock-in amplifier and therefore relatively longer acquisition time. In the present work, a detection method based on transient thermal response was developed for detection of gas mixtures on a microfabricated ultra-low-power microbridge TCD fabricated from polysilicon. A test bed and associated experiments were designed to evaluate the power consumption and speed of this technique compared with conventional steady-state measurements. To provide more insights into transient phenomena and predict μTCD behavior, an accurate multiphysics model was developed that is capable of simulating transient response of the sensor in a gas medium with minimal simplification. The developed technology is especially suitable for emerging ultra-portable and wireless gas analyzers in the internet-of-things era in which power consumption and footprint are critical criteria.

TRANSIENT THERMAL ANALYSIS OF MICRO-ELECTROTHERMAL GAS SENSOR

Figure 1 presents schematics of heat transfer components from the microbridge TCD. It has been shown that in the absence of forced convection and at temperatures of a few hundred degrees above ambient, the effects of radiation and natural convection from a μTCD are negligible[14]; as a result, conduction via gas medium is the dominant heat loss mechanism. Because of the high aspect ratio of the microbridge (on the order of 100:1), conduction along the bridge to the substrate, q_3, is smaller than

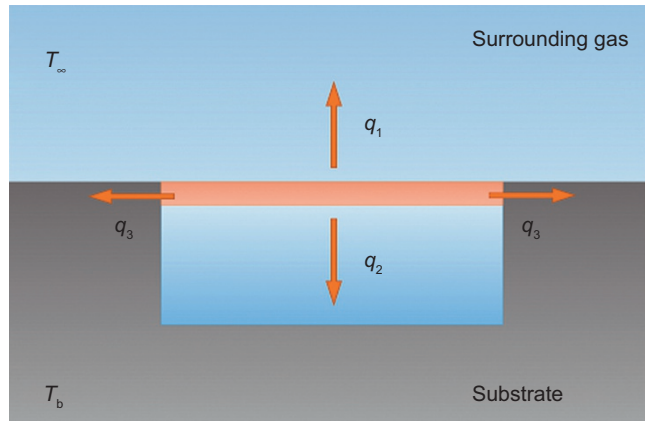

Figure 1 Schematics of heat dissipation from an electrothermal bridge.

conduction through the surrounding gas, q_1 and q_2. Additionally, conduction from below the microbridge, q_2, is expected to be larger than conduction from the top, q_1, because of the small gap between the microbridge and the relatively cool substrate. The overall major heat transfer from the bridge, $q_1 + q_2$, is a function of the thermal properties of the gas mixture. The small-mass microbridge is suspended in low-thermal-conductivity gases that make it capable of reaching high temperatures at very low power levels of few microwatts.

Even though the complex three-dimensional geometry of the microbridge makes it difficult to obtain an exact analytical solution of thermal phenomena, a lumped system analysis[15] can describe the relationship between sensor response, gas properties, and the applied power.

The lumped system method includes the assumption that temperature variations within an object can be neglected in thermal analyses whenever heat conduction within an object is much faster than heat transfer across the boundary of the object. This is a reasonable assumption for this case as the thermal conductivity of the silicon microbridge is three orders of magnitude larger than that of the surrounding gas medium. Therefore, spatial temperature variations within the object can be neglected in thermal analyses, although the average temperature of the microbridge used for lumped analysis can still vary over time.

At steady state, consideration of the energy balance implies that the rate of heat transfer from a lumped solid object is equal to the rate of heat generation within the object. For a high aspect ratio microbridge this can be written as:

$$\dot{Q} = k_f A \left.\frac{dT_f}{dy}\right|_{\text{wall}}$$

where $\dot{Q}$ is the rate of heat generation in the microbridge, k_f is the thermal conductivity of surrounding fluid, A is the surface area of the bridge, and $\left.\frac{dT_f}{dy}\right|_{\text{wall}}$ is the temperature gradient of the gas medium at the external surface of the bridge. Inserting the temperature of the microbridge, the ambient temperature T_∞ and a characteristic length of conduction, L, we can write:

$$\dot{Q} = k_f A \left.\frac{dT_f}{dx}\right|_{\text{wall}} \approx k_f A \frac{(T - T_\infty)}{L} \qquad (1)$$

The left-hand side of Equation (1) represents the dissipated electrical power I^2R, where I is the electric current and R is the resistance. For doped silicon, the temperature dependence of resistance can be described with a linear model as:

doi:10.1038/micronano.2015.25

$$R = R_0(1 + \alpha(T-T_{ref})) \quad (2)$$

where R_0 is the resistance of the conductor at reference temperature T_{ref} and α is the resistivity temperature coefficient. For easier analysis, let us choose $T_{ref} = T_\infty$ and then substitute $\dot{Q}$ in Equation (1) by electrical power dissipation; then:

$$I^2R_0(1 + \alpha(T-T_\infty)) = k_f A\frac{(T-T_\infty)}{L} \quad (3)$$

As Equation (3) describes, the temperature (and therefore the resistance) of the microbridge sensor at steady-state operation is related to the thermal conductivity of the gas medium at a certain input power. The left-hand side of the equation describes the electrical phenomena and first-order dependency on the temperature; the right-hand side represents conduction heat loss and is proportional to the average temperature of the microbridge. From this equation, the temperature change in the microbridge can be obtained as:

$$\frac{1}{T-T_\infty} = \frac{k_f}{I^2R_0}\left(\frac{A}{L}\right) - \alpha \quad (4)$$

At steady state, therefore, the inverse of the average temperature change of the microbridge is proportional to the effective thermal conductivity of the surrounding gas.

In a transient state (i.e., shortly after an electrical current step is applied to the sensor), the microbridge temperature rises from T_∞ to the hot steady-state operating temperature. By adding the transient term, Equation (3) is extended to:

$$I^2R_0(1 + \alpha(T-T_\infty)) = \rho VC_p\frac{dT}{dt} + k_f A\frac{(T-T_\infty)}{L} \quad (5)$$

where ρ is the density of the microbridge that serves as the dominant thermal mass in the system.

The time-resolved temperature solution is obtained from Equation (5) as:

$$T-T_\infty = \frac{I^2R_0}{k_f A/L - \alpha I^2R_0}(1-e^{-t/\tau}) \quad (6)$$

where τ is the time constant of heating and is defined as:

$$\frac{1}{\tau} = \frac{k_f A/L - \alpha I^2R_0}{\rho VC_p} \quad (7)$$

This analysis indicates that the time constant of heating is inversely proportional to the gas mixture thermal conductivity and the input power. The term ρVC_p represents the total thermal capacitance of the system and consists of two parts: that thermal mass of the solid material $\rho_s V_s C_s$ and the thermal mass of gas medium $\rho_g V_g C_g$. However, it is estimated that the thermal mass of the solid bridge is much larger than that of its surrounding gas. The parameter k_f is the effective thermal conductivity of the gas medium that is responsible for most of the heat lost from the bridge. A portion of the heat is conducted along the bridge to the solid substrate; as a result, the thermal conductivity of solid, k_s, plays a role. In analogy to electric circuits, Figure 2 presents a thermal circuit model for the microbridge sensor as a lumped system and provides insight on how the properties of solids and gases can affect sensor response. The resistors represent the thermal resistance of the gas and solid material and the capacitors represent the thermal capacitance of the system.

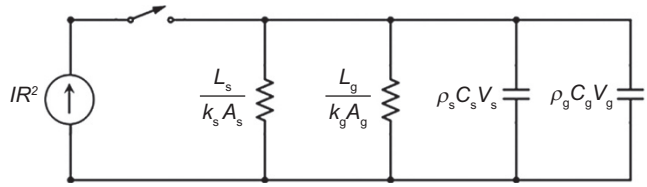

Figure 2 Thermal circuit for the microbridge sensor as a lumped system; subscript "s" indicates solid material properties and "g" corresponds to surrounding gas properties.

MATERIALS AND METHODS

Ultra-low power, superior sensitivity, and rapid response of the present sensor system were achieved through our newly developed μTCD. It consists of a 100-μm long microbridge fabricated from a 1×2 μm doped polysilicon layer and suspended using a silicon dioxide sacrificial layer. As shown in Figure 3a, the bridge is passivated with a relatively thin 200-nm silicon nitride layer to provide electrical isolation and protect the bridge against any reactions at hot temperatures. Doped polysilicon resistance changes at a relatively large rate with temperature and the average temperature of the bridge can be correlated to its resistance.

The fabrication process for this microbridge (i.e., the smallest polysilicon TCD) was described in our previous work[14] (see also Supplementary Figure S1). Figure 3b presents a scanning electron microscope image of a fabricated microbridge. Half of the microbridge at its center is fabricated to be narrower to locate more of the resistance and the generated heat at the center and away from the solid anchors.

Electrical characterization of the sensor was performed to determine base resistance R_0 and temperature coefficient of resistance α, for modeling and experiments. The sensor was placed in a temperature-controlled oven and subjected to a series of uniform steady temperatures up to 70 °C. For the microbridge in this study, a TCR of α = 0.00131/°C and a base resistance of R_0 = 3084 Ω at 23 °C were measured.

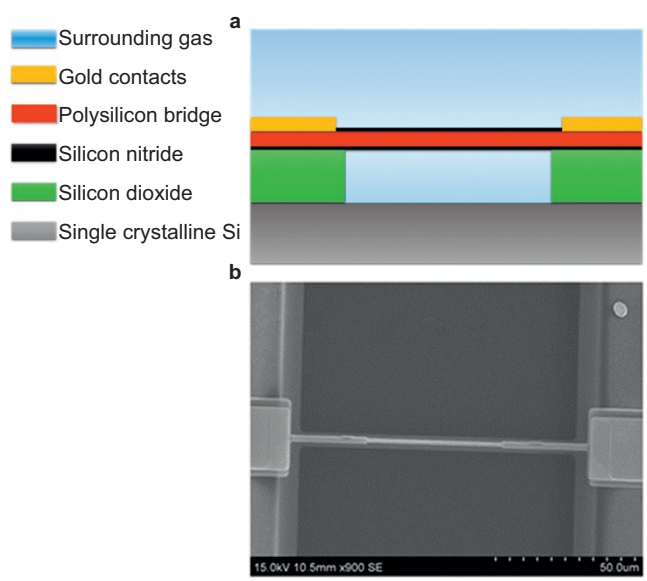

Figure 3 (**a**) Material composition of the suspended microbridge. (**b**) Scanning electron microscope image of the fabricated microsensor; a 100:1 bridge with 50:1 μm narrow center region.

For the experimental studies, a flow system was designed that was capable of accurately subjecting the sensor to the target concentrations of gas mixtures. Ambient air is composed of 79% nitrogen and its thermo-physical properties are very similar to nitrogen. Therefore, nitrogen was selected as the carrier gas for our experiments in controlled lab conditions. Each specific target concentration of an analyte was achieved by mixing the flow from a bottle of premixed 5% analyte in nitrogen with the flow from a pure nitrogen bottle as shown in Figure 4a. By adjusting the flows through two precise mass flow controllers (Alicat Scientific), analyte concentration can be controlled between 0% to 5%. The sensor was installed in a small glass container connected to the gas flow tubing and was placed inside an insulated oven to provide temperature stability and eliminate room temperature fluctuations. Before each measurement the sensor container was flushed with the desired gas mixture for 5 minutes. The total volumetric flow rate of 500 standard cubic centimeters per minute (sccm) was maintained during data collection to ensure that the mixture of gas did not change over time. Mixtures of helium, methane, carbon dioxide, and argon in nitrogen were tested.

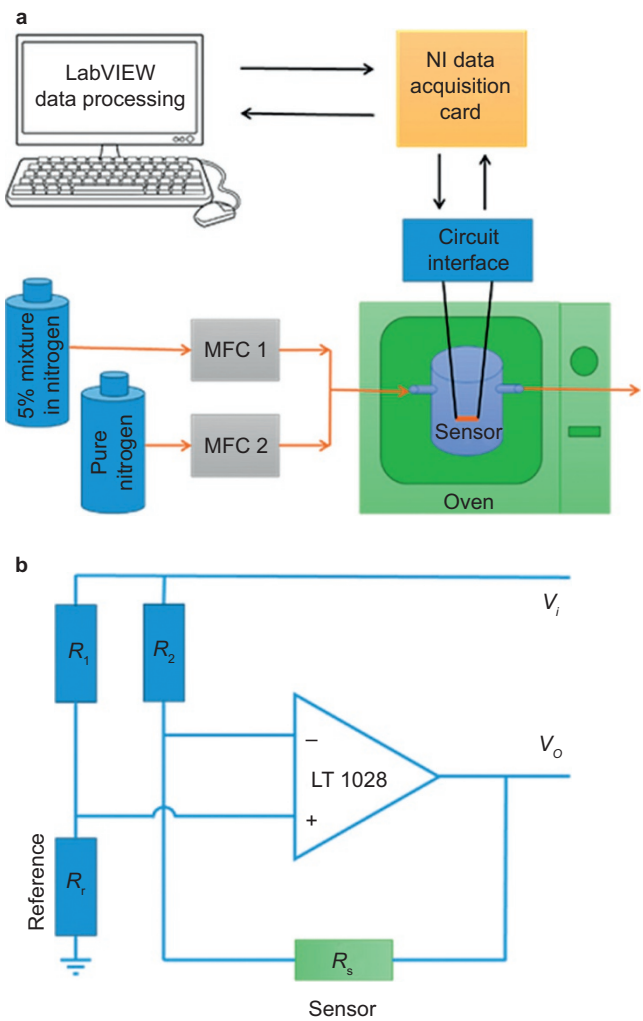

Figure 4 (**a**) Experimental setup including the flow system and data acquisition devices. (**b**) Circuit interface for the microbridge sensor to maintain constant current through the sensor and provide a measurable output voltage proportional to sensor resistance change.

For data acquisition, 16-bit analog-to-digital and digital-to-analog converters (National Instrument PCIe-6351, National Instruments, Austin, TX, USA) at a high sampling rate of 1 MS s^{-1} were employed. Serving as an interface between PC and the circuit interface, they were capable of generating waveforms for pulsed excitation of the sensor while simultaneously reading the analog output from the measurement system. A circuit interface was designed to apply pulses of constant current across the sensor and translate sensor resistance into an output voltage measurable by the data acquisition card. Conventionally, a Wheatstone bridge is employed for such MEMS sensors; however, it cannot maintain a constant current nor voltage over the sensor and therefore expresses nonlinear output at an extended range of measurements. Figure 4b shows a schematic of the circuit interface consisting of a reference resistor (R_r = 4 kΩ), two other auxiliary resistors (R_1 = 300 Ω), and an op-amp (Linear LT1028, Linear Technology, Milpitas, CA, USA). By changing the output voltage, V_o, the op-amp pulls a constant current through the sensor equal to the current passing through the reference resistor for a given input voltage of V_i. Therefore, the sensor resistance R_s can be obtained from Equation (8) as:

$$V_o = V_i \frac{R_r - R_s}{R_r + R_1} \tag{8}$$

When no electric current is applied, the microbridge rests at an ambient temperature and its resistance is at a minimum; this is referred to as a cold state and its corresponding resistance is referred to as a base resistance or cold resistance, R_0. The circuit can measure the base resistance by applying approximately 100 μA current and recording the corresponding V_o. During hot operation, V_o switches to a predefined high value and the microbridge temperature and its resistance increases; this state and the corresponding resistance are referred to as the hot state and hot resistance in this study.

Initial evaluations indicated that a continuous direct current at the hot state causes drifts in both the hot and cold resistance values of the sensor over time in a reversible manner. The drift indicates that the dissipated heat from DC excitation at the operating levels heats the sensor chip. To avoid this drift and more importantly obtain transient response of the sensor, square pulses were used instead of DC current (see Supplementary Figure S2 for sample of pulse train and output signals). Because the thermal mass of the microbridge is very low, it can reach steady-state hot temperature in less than 2 ms and provide one measurement sample. Experiments showed that a 50 Hz pulse with a duty cycle of 10% can prevent drift while providing 50 measurements per second, fast enough even for applications such as GC.

Although the average microbridge temperature can be calculated from its changing resistance, the temperature distributed over the bridge is not uniform. To obtain further insights into the heat transfer phenomena, reveal the temperature distribution and predictability of sensor time resolved response, a model of the microbridge was simulated in COMSOL 4.4 (COMSOL, Stockholm, Sweden). A detailed geometry of the composite bridge, obtained from scanning electron microscopy images, was used as a basis for the simulation. The model was meshed with 500,000 tetrahedral grid points that are fine (i.e., approximately 0.04 μm) at the bridge and smoothly get larger close to the outer boundaries where gradients vanish. Previously we have simulated flow and mass transfer phenomena using the open source tool OpenFOAM[16]; however, for the complex multiphysics and composite geometry of this problem, the more sophisticated software COMSOL was employed. Both solid materials and surrounding gas are included in the computational domain; therefore, no

doi:10.1038/micronano.2015.25

assumption and simplification was employed for thermal interaction between gas and solid surfaces. The computational domain is large and extended at least 200 μm from the bridge in each direction. In this method, the only thermal condition required on the domain outer boundaries is constant room temperature. As a wide range of temperatures are involved, properties of solids and gas are temperature-dependent and are taken into the account for further accuracy. Electrical and heat transfer physics are coupled in the model; the input current is provided as a boundary condition and the model handles heat generation, heat transfer, and resistance calculations simultaneously. Our previous simulation method[14] was developed further in this work to carry out a transient simulation with room temperature as the initial condition. Figure 5 presents the calculated steady-state temperature field under nitrogen at a power of I^2R_0 = 1.5 mW. The maximum local temperature occurs at the center of the microbridge and can reach 494 K, whereas the anchors remain at approximately substrate room temperature. The simulation results also verify that maximum local temperatures at the applied power is safe for sensor operation.

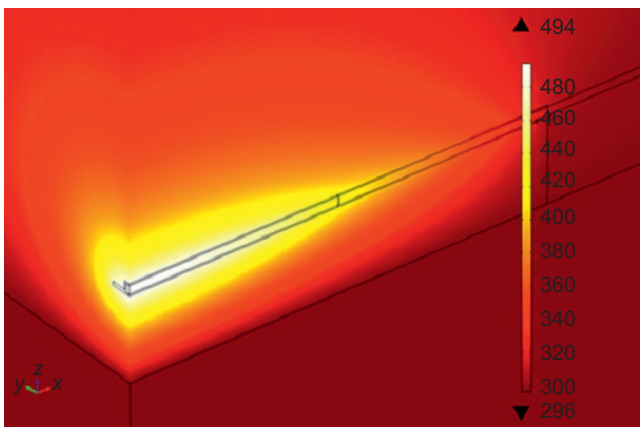

Figure 5 Steady-state temperature distribution in the microbridge and surrounding pure nitrogen at I^2R_0 = 1.5 mW. Only one quarter of the microbridge is shown because of the double plane symmetry. The leftmost part is the center of the bridge and the rightmost is the anchor.

RESULTS

Figure 6 presents a close look at the resistance change of the microbridge in nitrogen in response to a square current pulse of 0.7 mA and 2 ms width. The first few hundred microseconds of the response corresponds to the transient heating; this part is ignored in the steady-state measurements. Instead, the steady-state regime (in this case, the second millisecond of hot operation) is used for conventional operation. In this work we studied both transient and steady-state regimes for comparison.

According to our lumped system analysis, described in the previous section, it is expected that the microbridge resistance (i.e., its average temperature) behaves exponentially during a heating as Equation (9):

$$R = R_2 + (R_0 - R_2)e^{-t/\tau} \tag{9}$$

where R_0 is the base resistance, R_2 is the hot resistance, t is time, and τ is the time constant of the transient signal (i.e., the time required to achieve 63.2% of the total resistance change). The

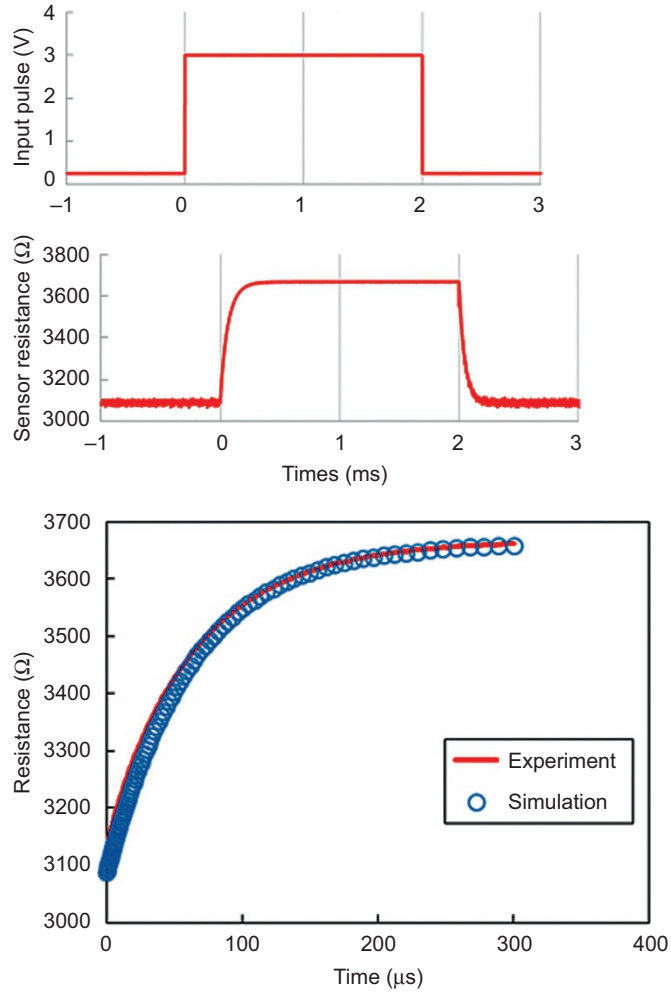

Figure 6 Experimental transient response of microbridge to a square pulse (left) and extracted heating curves for experiment and simulation (right).

time constant τ was obtained from experimental and simulation results by fitting an exponential curve using the least-squares method.

Figure 7 presents steady-state and transient microbridge response in pure nitrogen at three different power levels I^2R_0, where I is the high current value corresponding to the square excitation pulse train. As expected from our heat transfer analysis, $1/\tau$ varies linearly with power, whereas $1/\Delta R$ has an inverse relation with power. Both resistance change and τ are increased at higher powers and therefore the sensor can provide a better sensitivity at higher powers. However, for currents over 0.7 mA the sensor shows instabilities because of very high local temperatures; in practice, therefore, there is a limit to the input power. The trend of data coincides with the thermal analysis and suggests that at the lower end, as power approaches zero, ΔR approaches zero as well when τ is approaching a constant value.

Further experiments were conducted with gas mixtures at the higher power level of 1.5 mW. Figure 8 shows how the sensor responded to a change in concentration. A square current pulse of 50 Hz with a duty cycle of 10% (2 ms width) excited the microbridge. The transient time constant was extracted from the first 300 μs of the output pulse; simultaneously, the steady-state resistance change was calculated from the last 1 ms. The results

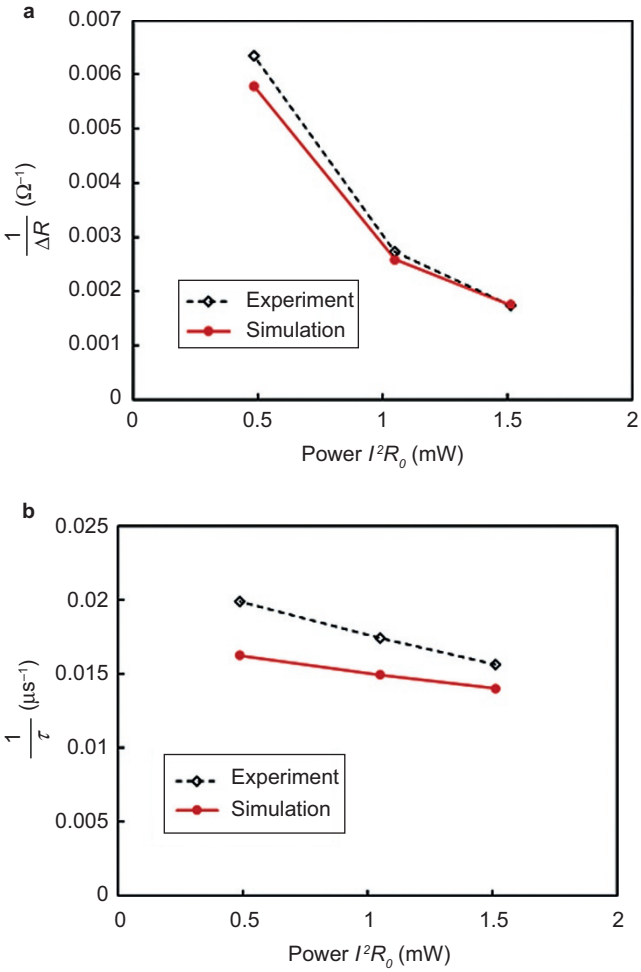

Figure 7 Experimental and simulation data for (**a**) steady-state resistance change and (**b**) time constant, at three different power levels in nitrogen.

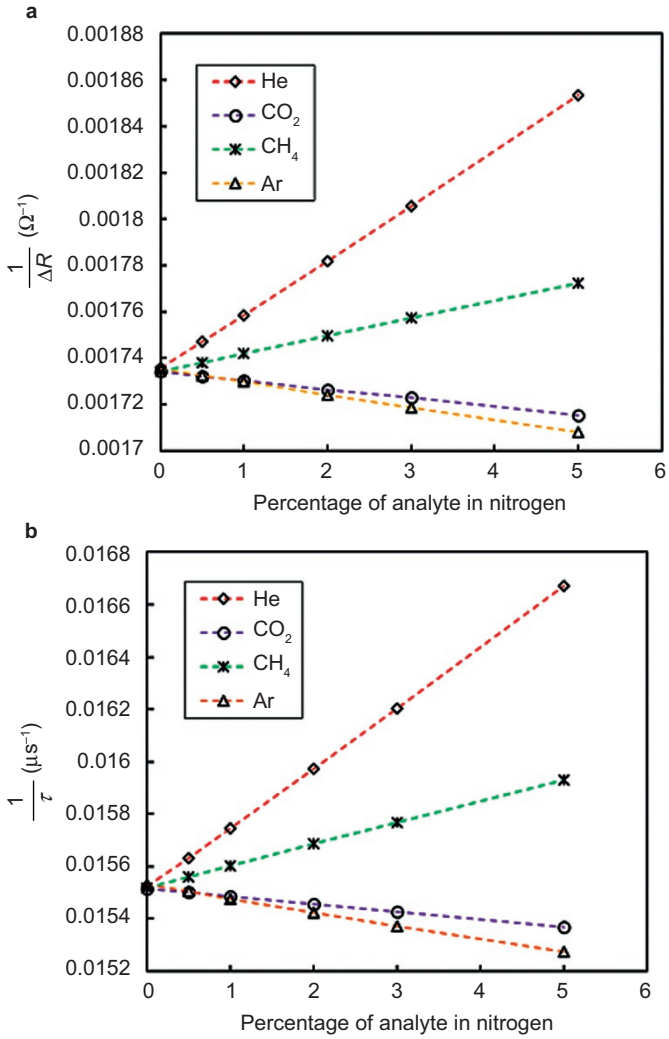

Figure 8 (**a**) Steady-state and (**b**) transient response of the sensor to mixtures of nitrogen with helium, carbon dioxide, methane, and argon. Analyte concentration was varied from 0 to 5%

were averaged over the course of 30 seconds to reduce electrical noise. Having the smallest thermal conductivity among those tested, helium exhibited the largest contrast with the nitrogen carrier. The same linear behavior was observed for both resistance values and time constant. Table 1 summarizes sensitivity and limit of detection for different gases in nitrogen. The limit of detection was calculated from sensitivity values along with standard deviation in resistance and time constant measurements, which were 0.015 Ω and 0.0022 μs, respectively. The reproducibility of the overall gas flow system and sensing system through multiple experiments was determined to be 0.25 Ω for the resistance and 0.035 μs for the time constant.

Table 1 Sensitivity and levels of detection for both steady-state resistance change and transient time constant

	Time constant sensitivity (ns/ppm)	Transient calculated limit of detection	Resistance sensitivity (mΩ/ppm)	Steady-state calculated limit of detection
Helium	−0.0889	25	−0.732	20
Methane	−0.0334	66	−0.248	60
Argon	0.0217	101	0.185	81
Carbon dioxide	0.0124	178	0.125	120

CONCLUSION AND DISCUSSION

In the present work a transient measurement method was implemented for a 100-μm long and 2-μm wide doped polysilicon microbridge. Thermal analysis and computer simulations demonstrated that the inverse transient time constant of the heating curve in response to an applied step current is proportional to thermal conductivity; therefore, it can be used for sensing purposes. Moreover, thermal analysis suggests that this time constant is independent of the baseline resistance. The new method was applied and tested for detection of gas mixtures and the results were compared with the conventional steady-state resistance readings. Data obtained for mixtures of helium, carbon dioxide, argon and methane, each in nitrogen, show that with using the same hardware, the transient method provides similar sensitivity with only 300 μs of sampling for a single measurement. In contrast, the steady-state measurements in this work required 800 μs of the steady-state response regime. A developed computer simulation of transient heating provided the temperature distribution in the microbridge and was able to predict the time constant of transient heating at different power levels.

An equivalent DC power of I^2R_0 = 1.5 mW was applied to the sensor, where I is the current value corresponding to the square

doi:10.1038/micronano.2015.25

excitation pulse train. Considering that a 50 Hz pulse train with 10% duty cycle was applied for excitation in this method and bringing the sensor resistance change into account, the sensor actual power consumption was approximately 180 nW (3.6 nJ per single measurement), which is the lowest reported power management on a TCD so far.

Efficient measurements do not arise from device design and microfabrication alone but also require the development of improved measurement methods and noise management. The lower power required in this method of operating this μTCD measurement system allows its integration into ultra-portable or wearable sensing devices. In addition, evolving miniature gas analyzer technologies such as micro-GC systems[17,18] demand the integration of highly efficient and fast micro-detectors, which could be another potential application for this technology.

ACKNOWLEDGEMENT

The authors would like to thank the funding and technical assistance from Georgia Tech Research Institute and KWJ Engineering Inc. The work was also sponsored by NASA, Samsung of America, and the U.S. Department of Energy. The sensor that was tested in this work is based on the patents: No. 7,911,010, No. 8,426,932 and No. 8,884,382.

COMPETING INTERESTS

The authors declare no conflicts of interest.

REFERENCES

1 Azad A, Akbar S, Mhaisalkar S *et al.* Solid-state gas sensors: A review. *Journal of the Electrochemical Society* 1992; **139**: 3690–3704.
2 Jones M, Nevell T. The detection of hydrogen using catalytic flammable gas sensors. *Sensors and Actuators* 1989; **16**: 215–224.
3 Zanini M, Visser J, Rimai L *et al.* Fabrication and properties of a Si-based high-sensitivity microcalorimetric gas sensor. *Sensors and Actuators A*: *Physical* 1995; **48**: 187–192.
4 Semancik S, Cavicchi R, Wheeler M *et al.* Microhotplate platforms for chemical sensor research. *Sensors and Actuators B*: *Chemical* 2001; **77**: 579–591.
5 Suehle JS, Cavicchi RE, Gaitan M *et al.* Tin oxide gas sensor fabricated using CMOS micro-hotplates and in-situ processing. IEEE *Electron Device Letters* 1993; **14**: 118–120.
6 Elmi I, Zampolli S, Cozzani E *et al.* Development of ultra-low-power consumption MOX sensors with ppb-level VOC detection capabilities for emerging applications. *Sensors and Actuators B*: *Chemical* 2008; **135**: 342–351.
7 Decarli M, Lorenzelli L, Guarnieri V *et al.* Integration of a technique for the deposition of nanostructured films with MEMS-based microfabrication technologies: Application to micro gas sensors. *Microelectronic Engineering* 2009; **86**: 1247–1249.
8 Puente D, Gracia FJ, Ayerdi I. Thermal conductivity microsensor for determining the methane number of natural gas. *Sensors and Actuators B*: *Chemical* 2005; **110**: 181–189.
9 Cruz D, Chang J, Showalter S *et al.* Microfabricated thermal conductivity detector for the micro-ChemLab™. *Sensors and Actuators B*: *Chemical* 2007; **121**: 414–422.
10 Mayer F, Salis G, Funk J *et al.* Scaling of thermal CMOS gas flow microsensors: Experiment and simulation. IEEE Proceedings of the Ninth Annual International Workshop on Micro Electro Mechanical Systems, 1996 (MEMS'96). An Investigation of Micro Structures, Sensors, Actuators, Machines and Systems. IEEE; 11–15 Feb 1996; San Diego, CA, USA; 1996: 116–121.
11 Moser D, Lenggenhager R, Wachutka G *et al.* Fabrication and modelling of CMOS microbridge gas-flow sensors. *Sensors and Actuators B*: *Chemical* 1992; **6**: 165–169.
12 Healy J, De Groot J, Kestin J. The theory of the transient hot-wire method for measuring thermal conductivity. *Physica B + C* 1976; **82**: 392–408.
13 Nagasaka Y, Nagashima A. Simultaneous measurement of the thermal conductivity and the thermal diffusivity of liquids by the transient hot-wire method. *Review of Scientific Instruments* 1981; **52**: 229–232.
14 Mahdavifar A, Aguilar R, Peng Z *et al.* Simulation and fabrication of an ultra-low power miniature microbridge thermal conductivity gas sensor. *Journal of the Electrochemical Society* 2014; **161**: B55–B61.
15 Incropera FP. Introduction to Heat Transfer. John Wiley & Sons, Hoboken, NJ, USA; 2011: 280–282.
16 Mahdavifar A, Pollard A, Pharoah J *et al.* Wall proximity effects on flow over a simple membrane spacer. *Computers & Fluids* 2013; **88**: 180–188.
17 Navaei M, Mahdavifar A, Dimandja JM *et al.* All silicon micro-GC column temperature programming using axial heating. *Micromachines* 2015; **6**: 865–878.
18 Navaei M, Mahdavifar A, Xu J *et al.* Micro-fabrication of all silicon 3 meter GC columns using gold eutectic fusion bonding. *ECS Journal of Solid State Science and Technology* 2015; **4**: S3011–S3015.

Supplementary information for this article can be found on the *Microsystems & Nanoengineering* website (http://www.nature.com/micronano).